Synthesis and Reactivity of Bimetallic Alkoxysilyl Complexes. Crystal Structure of $[Fe(CO)_3\{\mu\text{-}Si(OMe)_2(OMe)\}(\mu\text{-}dppm)Rh(CO)]$ (dppm = $Ph_2PCH_2PPh_2$): A Complex with a μ_2-η^2-SiO Bridge between Iron and Rhodium

Pierre Braunstein,* Michael Knorr, and Eva Villarroya

Laboratoire de Chimie de Coordination, Associé au CNRS (URA 0416), Université Louis Pasteur, 4 rue Blaise Pascal, F-67070 Strasbourg Cédex, France

André DeCian and Jean Fischer

Laboratoire de Cristallochimie et de Chimie Structurale, Associé au CNRS (UA 424), Université Louis Pasteur, 4 rue Blaise Pascal, F-67070 Strasbourg Cédex, France

Received February 28, 1991

Bimetallic Fe–Rh complexes have been prepared from the (alkoxysilyl)iron derivatives $[HFe(CO)_3\{Si(OMe)_3\}(dppm\text{-}P)]$ or $[HFe(CO)_3\{Si(OMe)_3\}(dppm\text{-}P)]^-$, the dppm ligand of which helps assembling and stabilizing the dinuclear unit. The crystal structure of $[Fe(CO)_3\{\mu\text{-}Si(OMe)_2(OMe)\}(\mu\text{-}dppm)Rh(CO)]$ (**1a**) has been determined: monoclinic, space group $P2_1/n$, a = 22.717 (5) Å, b = 11.348 (2) Å, c = 14.202 (2) Å, β = 94.47 (2)°, V = 3650.2 Å^3, Z = 4, R = 0.033, R_w = 0.052 for 4531 reflections with $I > 3\sigma(I)$. Complex **1a** contains an unusual μ_2-η^2-SiO bridge between the Fe and Rh atoms (Fe–Rh = 2.6283 (7), Rh–O7 = 2.167 (3), O7–Si = 1.683 (3), Si–Fe = 2.249 (1) Å). Complex $[Fe(CO)_3\{\mu\text{-}Si(OMe)_2(OMe)\}(\mu\text{-}dppm)Rh(PPh_3)]$ (**2**) reacts with $P(OPh)_3$ to give $[Fe(CO)_3\{\mu\text{-}Si(OMe)_2(OMe)\}(\mu\text{-}dppm)Rh\{P(OPh)_3\}]$ (**3**). Complex **1a** reacts reversibly with CO with opening of the μ_2-η^2-SiO bridge to give $[Fe(CO)_3\{Si(OMe)_3\}(\mu\text{-}dppm)Rh(CO)_2]$ (**4**). Protonation of the Fe–Rh bond of **1a** with HBF_4 yields $[Fe(CO)_2\{\mu\text{-}Si(OMe_2(OMe)\}(\mu\text{-}dppm)(\mu\text{-}H)(\mu\text{-}CO)Rh(PPh_3)][BF_4]$ (**5**), which is isoelectronic with $[Fe(CO)_2\{\mu\text{-}Si(OMe)_2(OMe)\}(\mu\text{-}dppm)(\mu\text{-}H)(\mu\text{-}CO)RhCl]$ (**6a**), prepared by the addition of $[HFe(CO)_3\{Si(OMe)_3\}(dppm\text{-}P)]$ to a suspension of $[Rh_2(\mu\text{-}Cl)_2(COD)_2]$ in Et_2O. Reaction of $K[Fe(CO)_3\{Si(OMe)_3\}(dppm\text{-}P)]$ with $[RhCl(CS)(PPh_3)_2]$ afforded $[Fe(CO)_3\{Si(OMe)_3\}(\mu\text{-}dppm)Rh(CS)(PPh_3)]$ (**8**). The stronger Rh–CS interaction compared with the Rh–CO interaction accounts for the strengthening of its bonding to Rh, preventing the transformation of **8** into **2**, and also of the Rh←PPh_3 bond, which precludes formation of the Rh–CS analogue of **1a**. In contrast to the rigid situation in **1a**, the lability of the O→Rh bond in **2**, **3**, **5**, and **6** accounts for the dynamic behavior of the alkoxysilyl ligand, evidenced by variable-temperature ^1H NMR spectroscopy, which renders the methoxy protons equivalent. The observed increase in O→Rh bond lability parallels the increase in electron density at the Rh center. Attempts to isolate related Fe–Co or Fe–Ir complexes were unsuccessful. In the latter case, a redox reaction resulted in the formation of $[Fe(CO)_3(PPh_3)(dppm\text{-}P)]$.

Introduction

We have recently described reactions of the hydrido complex $[HFe(CO)_3\{Si(OMe)_3\}(dppm\text{-}P)]$ (dppm = $Ph_2PCH_2PPh_2$) and the related salts $K[Fe(CO)_3\{Si(OR)_3\}(dppm\text{-}P)]$ (R = Me, Et) with a variety of metal reagents.[1-4] One aspect of this work has involved the synthesis of heterometallic complexes in which the alkoxysilyl group, σ-bonded to iron, experiences an unprecedented μ_2-η^2-SiO bonding mode via donation of an oxygen lone pair to the neighboring metal center, as depicted in A. For example, reactions between the complexes $K[Fe(CO)_3\{Si(OMe)_3\}(dppm\text{-}P)]$ and $MCl_2(PhCN)_2$ (M = Pd, Pt) have yielded $Fe(CO)_3\{\mu\text{-}Si(OMe)_2(OMe)\}(\mu\text{-}dppm)MCl$. When M = Pd, the O→Pd bond, of length 2.100 (4) Å, was found to dissociate in solution (^1H NMR evidence). However, we could obtain no evidence for the formation of products resulting from nucleophilic displacement of this O→Pd bond by a donor ligand such as CO or PPh_3.[1] The unusual features associated with the (hard) oxygen-(soft) metal interaction in the MFeSiO four-membered ring and its possible relevance to the stabilization of co-

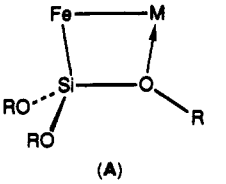

(A)

(1) Braunstein, P.; Knorr, M.; Tiripicchio, A.; Tiripicchio Camellini, M. *Angew. Chem., Int. Ed. Engl.* **1989**, *28*, 1361.
(2) Braunstein, P.; Knorr, M.; Villarroya, E.; Fischer, J. *New J. Chem.* **1990**, *14*, 583.
(3) Braunstein, P.; Knorr, M.; Piana, H.; Schubert, U. *Organometallics* **1991**, *10*, 828.
(4) Braunstein, P.; Knorr, M.; Schubert, U.; Lanfranchi, M.; Tiripicchio, A. *J. Chem. Soc., Dalton Trans.* **1991**, 1507.

0276-7333/91/2310-3714$02.50/0

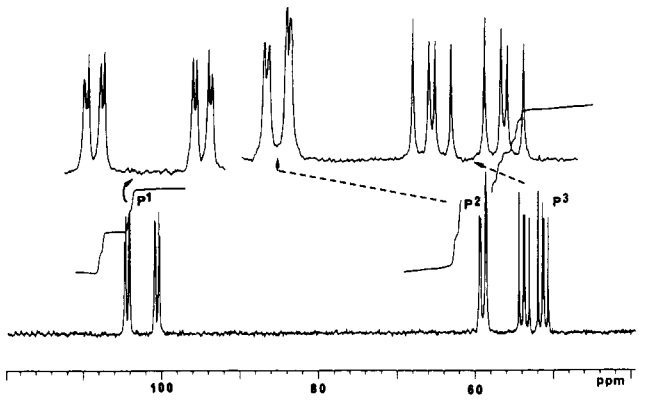

Figure 1. $^{31}P\{^1H\}$ NMR spectrum of $[Fe(CO)_3\{\mu\text{-}Si(OMe)_2(OMe)\}(\mu\text{-dppm})Rh\{P(OPh)_3\}]$ (**3**).

ordinatively unsaturated, reactive molecular or surface species, prompted us to examine other bimetallic systems with the aim of relating the nature of the O→M interaction, and the associated "hemilabile" behavior of the $Si(OR)_3$ ligand, with the nature of M and the charge of the complex (e.g., neutral or cationic). The dinuclear unit required for the occurrence of this unprecedented μ_2-η^2-SiO bonding mode may be conveniently generated and stabilized through the assistance of the dppm ligand. We now report the preparation of a series of Fe–Rh complexes and describe the crystal structure of $[Fe(CO)_3\{\mu\text{-}Si(OMe)_2(OMe)\}(\mu\text{-dppm})Rh(CO)]$ (**1a**) whose synthesis has been reported recently.[2]

Results and Discussion

The assistance of the dppm ligand in generating and stabilizing metal–metal-bonded heterodinuclear complexes was further exploited in this work. The hydridoiron complexes $[HFe(CO)_3\{Si(OR)_3\}(dppm\text{-}P)]$ and the corresponding metalates possess a monodentate dppm ligand and are suitable reagents for the synthesis of heterometallic Fe–Rh complexes. The pendent phosphorus donor atom of monodentate dppm Fe complexes has already been used for the synthesis of Fe–Rh complexes.[5a,b] Complex **1a** is conveniently prepared by the reaction of $K[Fe(CO)_3\{Si(OMe)_3\}(dppm\text{-}P)]$ with $[Rh(\mu\text{-}Cl)(CO)_2]_2$.[2] For comparison, we prepared in an analogous manner the bright yellow derivative $[Fe(CO)_3\{\mu\text{-}Si(OEt)_2(OEt)\}(\mu\text{-dppm})Rh(CO)]$ (**1b**). The spectroscopic features for this compound, in particular the ^1H NMR spectrum (vide infra), indicate also in this case the presence in solution of a rigid RhFeSiO four-membered ring system at ambient temperature. Complex **1a** is also formed, in quantitative spectroscopic yields (IR monitoring), by the reaction of eq 1a, which occurs within 0.5 h under mild conditions. Although **1a** reacts with PPh_3 to form **2** (eq 1b), this reaction is slower than that of eq 1a and therefore does not prevent isolation of pure **1a** when prepared according to eq 1a.

The results of the crystal structure determination of **1a** (see below) are consistent with the solution data, which indicated the existence of a rigid (on the ^1H and ^{13}C NMR time scales) MeO→Rh dative interaction. Complex **2** (eq

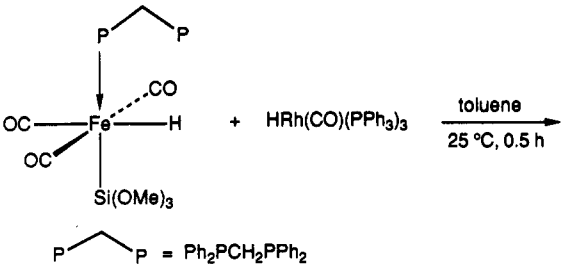

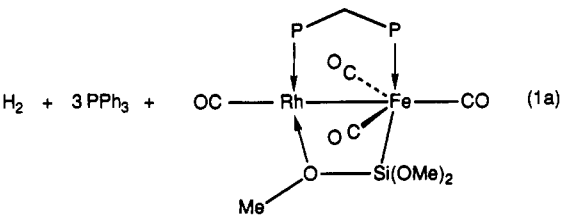

1a

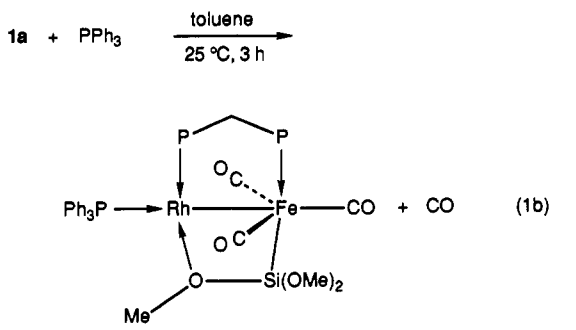

2

1b) may be formed from **1a** but is best prepared by the direct reaction of $K[Fe(CO)_3\{Si(OMe)_3\}(dppm\text{-}P)]$ with $[RhCl(PPh_3)_3]$ (eq 2). It is noteworthy that this complex

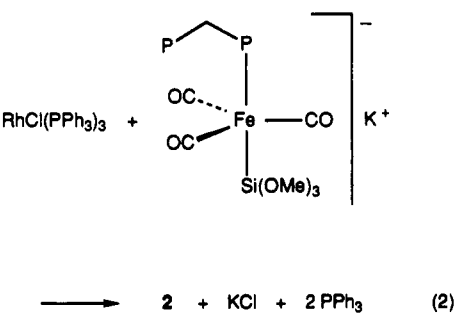

also forms in the reaction of eq 3, which was carried out with the hope that intermolecular HCl elimination would lead to a bimetallic complex containing a $Si(OMe)_3$ ligand on each metal center. However, reductive elimination of silane from the Rh(III) center occurred instead, followed by HCl elimination and formation of the Fe–Rh bond. These steps are substantiated by previous observations that $[HRhCl\{Si(OEt)_3\}(PPh_3)_2]$ rapidly reacts with, e.g., $PMePh_2$ under elimination of silane.[6] In our case, the pendent phosphorus atom of $[HFe(CO)_3\{Si(OMe)_3\}(dppm\text{-}P)]$ would play a similar role. The subsequent HCl elimination reaction is similar to that previously observed between $[HFe(CO)_3\{Si(OMe)_3\}(dppm\text{-}P)]$ and $[PdCl_2(PhCN)_2]$.[1]

Like complex **1**, **2** displays a μ_2-η^2-SiO bridge between the metals, as evidenced by the two ^1H NMR resonances

(5) (a) Jacobsen, G. B.; Shaw, B. L.; Thornton-Pett, M. *J. Chem. Soc., Dalton Trans.* **1987**, 2751. (b) Shaw, B. L.; Smith, M. J.; Stretton, G. N.; Thornton-Pett, M. *Ibid.* **1988**, 2099. (c) Haines, R. J.; Steen, N. D. C. T., English, R. B., *Ibid.* **1983**, 1607. (d) King, M.; Holt, E. M.; Radnia, P.; McKennis, J. S. *Organometallics* **1982**, *1*, 1718.

(6) Haszeldine, R. N.; Parish, R. V.; Taylor, R. J. *J. Chem. Soc., Dalton Trans.* **1974**, 2311.

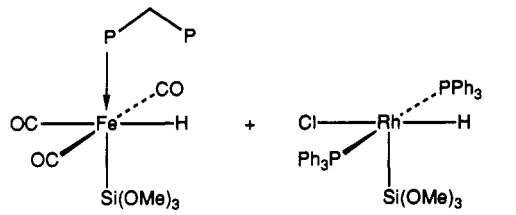

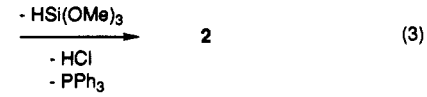

(3)

for the methoxy protons, at δ 2.36 and 3.78, in a 1:2 relative ratio, respectively. The $^{31}P\{^1H\}$ NMR spectrum of this complex contains three sets of resonances. The doublet of doublets at δ 58.3 corresponds to the Fe-bound phoshorus atom, which is coupled to the other dppm phosphorus atom with a J(PP) value of 61 Hz (which is in the range found for Fe–Pd, Fe–Pt, and Fe–Ag complexes displaying this μ_2-η^2-SiO bridge),[1-4] and to the PPh_3 ligand with a ^3J(PP) value of 6 Hz. The dppm phosphorus atom bonded to Rh appears at δ 54.4 as a ddd pattern, owing to coupling to Rh (^1J(P2–Rh) = 208 Hz) and to the other two phosphorus nuclei. Finally, the resonance for the PPh_3 ligand appears around δ 30 as a ddd pattern (^1J(P3–Rh) = 175 Hz). This complex is air stable in the solid state but slowly (in the course of few hours) decomposes in solution, even under nitrogen, with formation of **1a**. Although **2** does not react with phenylacetylene in CH_2Cl_2 at room temperature, it leads to quantitative formation of **3** upon reaction with a slight excess of $P(OPh)_3$ in

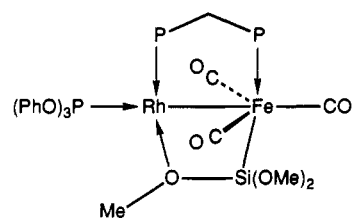

3

toluene at room temperature. The $^{31}P\{^1H\}$ NMR spectrum of this complex is very informative (Figure 1 and the Experimental Section) and confirms the structure drawn. It consists again of three sets of resonances, corresponding to mutually coupled phosphorus atoms, two of which show typical values for ^1J(P–Rh) coupling.[7] The shift toward higher frequencies of the ν(CO) vibrations is consistent with the expected decreased electron density at the iron center when compared with **2**. Complexes **1** and **2** react rapidly with CO to form $[Fe(CO)_3\{Si(OMe)_3\}(\mu\text{-dppm})Rh(CO)_2]$ (**4**) in which the Si–O bridge has been displaced by CO (eq 4). This is conveniently monitored in cyclo-

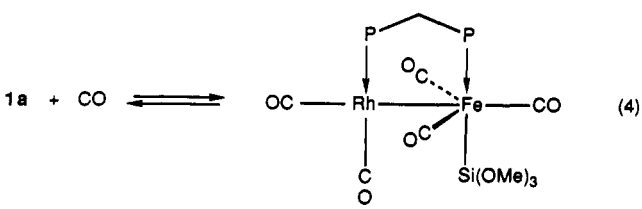

(4)

hexane solution by IR spectroscopy in the ν(CO) region where the bands of **1a** (1984, 1959, 1905, 1874 cm^{-1}) are replaced by those of **4** (2051, 1995, 1980, 1947, 1931 cm^{-1}). The ^1H NMR spectrum contains only a singlet resonance for the methoxy protons, even at 253 K, indicating that rupture of the O→Rh bond has occurred. The $^{31}P\{^1H\}$ NMR spectrum of **4** contains a singlet at δ 65.3 assigned to the Fe-bound P atom and a doublet at δ 15.5 (^1J(RhP) = 81 Hz), owing to a J(PP) coupling being accidentally close to zero. Purging a solution of **4** in CH_2Cl_2 with N_2 regenerates **1** quantitatively, and solid **4** was therefore crystallized from a CO-saturated solution. The behavior of this complex is at variance with that of the Fe–Pd complex $[Fe(CO)_3\{\mu\text{-}Si(OMe)_2(OMe)\}(\mu\text{-dppm})PdCl]$, which did not react with CO under similar conditions,[1] despite its Si–O bridge being labile on the NMR time scale.

Addition of excess HBF_4 to a CH_2Cl_2 solution of **2** at −40 °C resulted in instantaneous, quantitative protonation of the complex to afford $[Fe(CO)_2\{\mu\text{-}Si(OMe)_2(OMe)\}(\mu\text{-dppm})(\mu\text{-H})(\mu\text{-CO})Rh(PPh_3)][BF_4]$ (**5**) (eq 5). Its IR

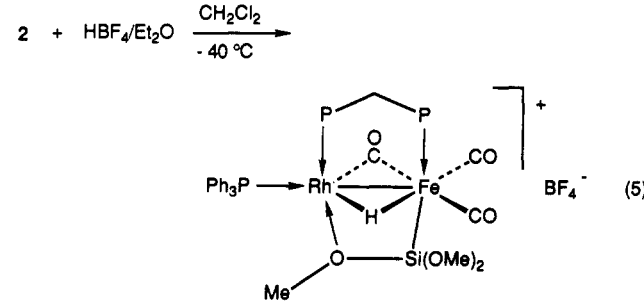

(5)

5

spectrum contains three ν(CO) absorptions at 2034, 1986, and 1827 cm^{-1}, the latter indicating the presence of a bridging carbonyl ligand. The hydride resonance in the ^1H NMR spectrum appears at δ −14.2 as a symmetrical, complex multiplet owing to coupling to all phosphorus atoms and to rhodium, consistent with its bridging the metal–metal bond. The presence of these bridging ligands destroys the pseudo mirror plane found in **2** (plane Fe, Rh, P, P) and accounts for the observation at 243 K of three distinct resonances for the chemically and magnetically inequivalent methoxy protons. In the $^{31}P\{^1H\}$ NMR spectrum of this complex, the resonance of the Fe-bound dppm phosphorus atom is significantly shifted to higher fields (δ ~38) when compared with that in **2** (δ ~58).

The reaction of $[HFe(CO)_3\{Si(OMe)_3\}(dppm\text{-}P)]$ with $[Rh_2(\mu\text{-Cl})_2(COD)_2]$ afforded in high yields another hydrido, carbonyl-bridged Fe–Rh complex, $[Fe(CO)_2\{\mu\text{-}Si(OMe)_2(OMe)\}(\mu\text{-dppm})(\mu\text{-H})(\mu\text{-CO})RhCl]$ (**6a**) that was fully characterized by analytical and spectroscopic methods (eq 6). The bridging position of the hydride ligand is deduced from the observation in the ^1H NMR spectrum at 218 K of a doublet of triplets at δ −15.86 (^2J(PH) = 15.1 and ^1J(HRh) = 26.2 Hz). The diastereotopic methylene protons give rise to a complex multiplet owing to further coupling with the phosphorus and rhodium atoms. The corresponding bromo and iodo derivatives **6b** and **6c** were obtained by reaction of **6a** with NaBr and NaI in THF, respectively. The ^1H NMR spectrum of these complexes at ambient temperature contains only a singlet resonance for the methoxy protons, discussed below. Spectroscopic IR and ^1H NMR monitoring showed that **6c** was also formed in the reaction of **1** with HI in CH_2Cl_2. Complexes

(7) Pregosin, P. S. *Phosphorus-31 NMR Spectroscopy in Stereochemical Analysis*; VCH: New York, 1987; pp 465–530.

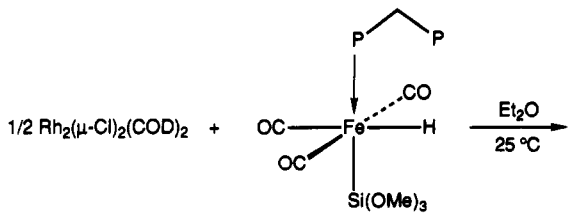

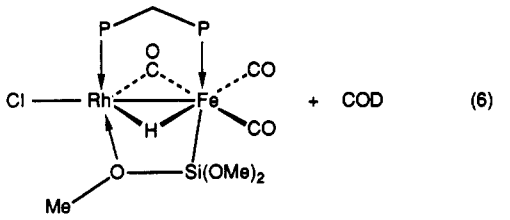

6a

6 are isoelectronic with the Ru–Rh complex $[RuRhH_2Cl(CO)_2(dppm)_2]$, which also exhibits bridging hydrido and carbonyl ligands.[8] Complex **6a** reacted rapidly with CO (disappearance of the ν(CO) vibration at 1793 cm^{-1}) to give a Fe–Rh species (**7**), not fully identified, that contains a (bridging) hydride ligand (δ −6.41 (ddd) at 298 K) and a terminal $Si(OMe)_3$ group (δ 3.78 (s)). Its ^1J(RhH) coupling constant of 21.9 Hz is similar to that of 24.5 Hz found in the square pyramidal Rh(III) complex $[HRhCl\{Si(OMe)_3\}_2(PPh_3)_2]$ (hydride resonance at δ −14.8 (dt) with ^2J(PH) = 14 Hz). The CH_2 protons of the dppm ligand of **7** appear as a triplet in the ^1H NMR spectrum with a J(PH) coupling of 12 Hz. The $^{31}P\{^1H\}$ NMR spectrum contains a doublet at δ 63.1 (J(PP) = 73 Hz) and a doublet of doublets at δ 44.8 (^1J(RhP) = 148 Hz). A tentative structure is drawn for **7**. This complex decomposes within

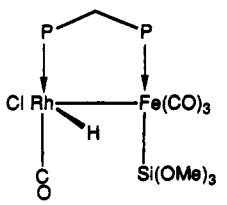

7

ca. 1 h in solution under reductive elimination of $HSi(OMe)_3$ [^1H NMR (benzene-d_6): δ 3.36 (OMe, 9 H), 4.46 (SiH)] and formation of a yet unidentified complex that contains dppm [^1H NMR (benzene-d_6): δ 2.77 (t, ^2J(PH) = 10 Hz)]. Reductive elimination of silane induced by CO has already been reported for mononuclear complexes,[9] and it often involves nonclassical Si–H interactions (2e–3c).[10]

In order to obtain an Fe–Rh–CS complex analogous to **1a**, the reaction of $K[Fe(CO)_3\{Si(OMe)_3\}(dppm\text{-}P)]$ with $[RhCl(PPh_3)_2(CS)]$ was carried out in THF (eq 7). Yellow-orange microcrystals of **8** were isolated in ca. 78% yield. Surprisingly, a PPh_3 ligand has remained attached to Rh and was shown by $^{31}P\{^1H\}$ NMR to occupy a position cis to the Rh-bound dppm phosphorus (^2J(PP) = 12 Hz). The methoxy resonance appears as a singlet (δ 3.62), in-

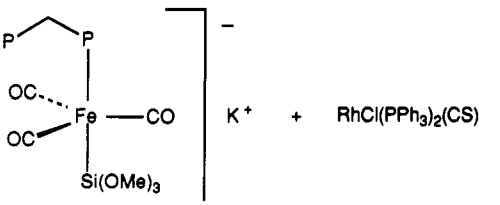

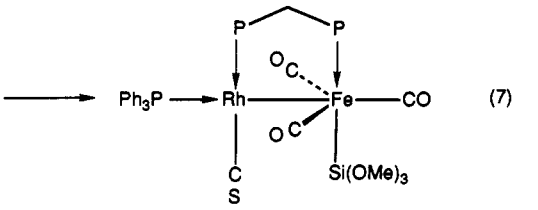

8

dicating for this complex a structure analogous to that of **4**. It is also related to the structure of $[Fe(CO)_3\{Si(OMe)_3\}(\mu\text{-dppm})Pt(H)(PPh_3)]$ in which the Pt–H unit replaces the Rh–CS moiety of **8**, both complexes having a PPh_3 ligand in a trans position with respect to the metal–metal bond. The ν(CS) vibration is shifted from 1300 cm^{-1} in $[RhCl(PPh_3)_2(CS)]$[11] to 1190 cm^{-1} in **8**, as a result of increased back-donation from rhodium. The stronger π-accepting properties of CS vs CO account for the strengthening of its bonding to Rh, preventing the transformation of the complex into **2**, and also of the Rh←PPh_3 bond, which precludes formation of the Rh–CS analogue of **1a**. When a CH_2Cl_2 solution of this compound was purged with CO for 10 min, no spectral change occurred.

In contrast to the reaction of $K[Fe(CO)_3\{Si(OMe)_3\}(dppm\text{-}P)]$ with $[RhCl(PPh_3)_3]$ (eq 2), that with $[CoCl(PPh_3)_3]$ (THF, −78 to +20 °C, 0.5 h) failed to give a dinuclear complex ($^{31}P\{^1H\}$ NMR analysis of the reaction mixture). Attempts to isolate Fe–Ir complexes displaying an IrFeSiO unit were also unsuccessful. Thus, although the reaction of *mer*-$[HFe(CO)_3\{Si(OMe)_3\}(dppm\text{-}P)]$ with $[Ir(\mu\text{-}Cl)(COD)]$ rapidly proceeded at 0 °C with formation of a dinuclear complex ($^{31}P\{^1H\}$ NMR monitoring showed the presence of only one P-containing product with δ(P(Fe)) = 58.0 (d, J(PP) = 70 Hz) and δ(P(Ir)) = 11.8 (dd)), no evidence was found for a MeO→Ir dative interaction. The lability of this complex prevented its full characterization. Likewise, reaction of $K[Fe(CO)_3\{Si(OMe)_3\}(dppm\text{-}P)]$ with $[IrCl(CO)_2(p\text{-toluidine})]$ led to no isolable Fe–Ir complex. Upon addition of $K[Fe(CO)_3\{Si(OMe)_3\}(dppm\text{-}P)]$ to a THF solution of $[IrCl(CO)(PPh_3)_2]$, a redox reaction took place, as shown by the formation of the Fe(0) complex $[Fe(CO)_3(PPh_3)(dppm\text{-}P)]$ as the main product. The latter complex, which does not appear to have been reported before, was characterized by analytical and spectroscopic methods (see the Experimental Section). Futhermore, $^{31}P\{^1H\}$ NMR examination of the crude reaction mixture revealed, in addition to two singlets at δ 24.1 (unreacted $[IrCl(CO)(PPh_3)_2]$) and δ −0.2, an AX pattern at δ 44.5 and −22.2 (J(PP) = 86 Hz), indicating the presence of a dppm-bridged Fe–Ir complex as a minor product (ca. 10% yield as determined by $^{31}P\{^1H\}$ NMR peak integration). It is interesting to note that bimetallic dppm complexes of Ir with Mn[12a] or Ru[12b] have also been

(8) Chaudret, B.; Delavaux, B.; Poilblanc, R. *Nouv. J. Chim.* **1983**, *7*, 679.
(9) (a) Aylett, B. J. *Adv. Inorg. Radiochem.* **1982**, *25*, 1. (b) Bellachioma, G.; Cardaci, G.; Colomer, E.; Corriu, R. J. P.; Vioux, A. *Inorg. Chem.* **1989**, *28*, 519.
(10) (a) Schubert, U. *Adv. Organomet. Chem.* **1990**, *30*, 151. See also: (b) McDonald, R.; Cowie, M. *Organometallics* **1990**, *9*, 2468.
(11) Baird, M. C.; Wilkinson, G. *J. Chem. Soc. A* **1967**, 2037.
(12) (a) Carr, S. W.; Shaw, B. L. *Polyhedron* **1987**, *6*, 111. (b) Delavaux, B.; Chaudret, B.; Devillers, J.; Dahan, F.; Commenges, G.; Poilblanc, R. *J. Am. Chem. Soc.* **1986**, *108*, 3703.

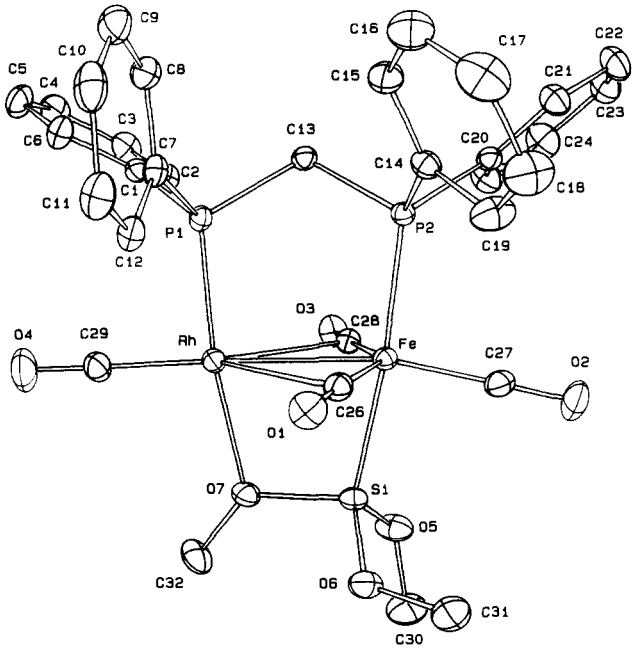

Figure 2. ORTEP plot of one molecule of $[Fe(CO)_3\{\mu\text{-}Si(OMe)_2(OMe)\}(\mu\text{-dppm})Rh(CO)]$ (**1a**) showing the numbering scheme used. Ellipsoids are scaled to enclose 50% of the electronic density. Hydrogen atoms are omitted.

Table I. Selected Bond Distances (Å) in $[Fe(CO)_3\{\mu\text{-}Si(OMe)_2(OMe)\}(\mu\text{-dppm})Rh(CO)]$ (1a)

	distance[a]		distance[a]
Rh–Fe	2.6283 (7)	C13–P2	1.830 (4)
Rh–P1	2.195 (1)	P2–C14	1.818 (5)
Rh–C26	2.692 (5)	P2–C20	1.842 (4)
Rh–C28	2.516 (4)	C26–O1	1.151 (6)
Rh–C29	1.839 (5)	C27–O2	1.153 (6)
Rh–O7	2.167 (3)	C28–O3	1.168 (5)
Fe–P2	2.213 (1)	C29–O4	1.144 (6)
Fe–C26	1.785 (5)	Si–O5	1.630 (4)
Fe–C27	1.759 (5)	Si–O6	1.627 (3)
Fe–C28	1.759 (5)	Si–O7	1.683 (3)
Fe–Si	2.249 (1)	O5–C30	1.414 (6)
P1–C1	1.827 (4)	O6–C31	1.425 (7)
P1–C7	1.812 (5)	O7–C32	1.418 (6)
P1–C13	1.844 (4)		

[a] Numbers in parentheses are estimated standard deviations in the least significant digits.

observed to be more labile than their Rh counterparts.

Crystal Structure of $[Fe(CO)_3\{\mu\text{-}Si(OMe)_2(OMe)\}(\mu\text{-dppm})Rh(CO)]\cdot CH_2Cl_2$ (1a·CH_2Cl_2). The bimetallic complex crystallizes with one molecule of CH_2Cl_2. The X-ray structure determination establishes the presence of a μ_2-η^2-SiO bridge between the metal centers. Figure 2 shows a perspective view of the molecular structure of **1a**, and relevant bond lengths and angles are given in Tables I and II, respectively. The geometry about the Fe atom is that of a distorted trigonal bipyramid in which P2 and Si occupy the apical sites. The P2–Fe–CO and Si–Fe–CO angles range between 93.9 (1)–95.2 (2) and 83.9 (1)–90.1 (2)°, respectively. The Fe–C–O angles, between 174.1 (4) and 178.7 (5)°, are indicative of terminal carbonyl ligands. This arrangement is as generally observed in this type of complex.[1-4] The geometry about Rh is square planar, with the carbonyl ligand C29–O4 trans to the Fe–Rh bond (Fe–Rh–C29 = 174.6 (2)°) and O7 trans to the P1 atom of the bridging dppm ligand (P1–Rh–O7 = 171.5 (1)°). We believe that the Rh–C26 and Rh–C28 distances of 2.692 (5) and 2.516 (4) Å result more from the geometry about the Fe atom than from significant semibridging interactions.[5b] The Fe–Rh distance of 2.6283 (7) Å is in a range normally associated with Fe–Rh single bonds.[5] The most significant feature in this structure is the presence of a μ_2-η^2-SiO bridge. The Rh–O7 distance of 2.167 (3) Å is shorter than the Rh–O(ether) distances of 2.201 (6) and 2.398 (5) Å in a Rh(II) complex,[14a] or the Rh–O distance of 2.249 (13) Å in a dinuclear Rh(II) methanol complex,[14b] but it is slightly longer than the Rh–O distances of 2.115 (5) and 2.130 (6) Å in Rh(I) aquo complexes.[14c] Rhodium–alkoxy distances are, as expected, much shorter (2.081 (4), 2.013 (1) Å).[15] The Rh–O7 distance is comparatively longer than the corresponding Pd–O distance of 2.100 (4) Å in the isoelectronic complex $[Fe(CO)_3\{\mu\text{-}Si(OMe)_2(OMe)\}(\mu\text{-dppm})PdCl]$.[1] However, variable-temperature NMR studies (see below) are consistent with a Pd(II)←O bond being more labile than the Rh(I)←O bond in these complexes.

As a result of the O7→Rh dative interaction, the Si–O7 bond of 1.683 (3) Å is elongated by comparison with the Si–O5 and Si–O6 bonds of 1.630 (4) and 1.627 (3) Å, respectively. A similar effect has also been observed in two Fe–Pd complexes where such a μ_2-η^2-SiO bridge has been characterized by X-ray diffraction.[1,3] The 16e rhodium and 18e iron centers in **1a** are best viewed as in the formal

Table II. Selected Bond Angles (deg) in $[Fe(CO)_3\{\mu\text{-}Si(OMe)_2(OMe)\}(\mu\text{-dppm})Rh(CO)]$ (1a)

	angle[a]		angle[a]
Fe–Rh–P1	93.02 (3)	C26–Fe–Si	84.0 (1)
Fe–Rh–C26	39.2 (1)	C27–Fe–C28	109.2 (2)
Fe–Rh–C28	39.9 (1)	C27–Fe–Si	90.1 (2)
Fe–Rh–C29	174.6 (2)	C28–Fe–Si	83.9 (1)
Fe–Rh–O7	78.86 (9)	C1–P1–C7	105.2 (2)
P1–Rh–C26	94.4 (1)	C1–P1–C13	101.5 (2)
P1–Rh–C28	92.1 (1)	C7–P1–C13	103.2 (2)
P1–Rh–C29	88.6 (2)	Rh–C26–Fe	68.5 (1)
P1–Rh–O7	171.51 (9)	Rh–C26–O1	113.4 (3)
C26–Rh–C28	79.1 (1)	Fe–C26–O1	177.4 (4)
C26–Rh–C29	135.5 (2)	Fe–C27–O2	178.7 (5)
C26–Rh–O7	80.9 (1)	Rh–C28–Fe	73.5 (2)
C28–Rh–C29	145.3 (2)	Rh–C28–O3	112.3 (3)
C28–Rh–O7	80.1 (1)	Fe–C28–O3	174.1 (4)
C29–Rh–O7	99.7 (2)	Rh–C29–O4	176.5 (5)
Rh–Fe–P2	98.24 (3)	P1–C13–P2	112.8 (2)
Rh–Fe–C26	72.3 (1)	C13–P2–C14	106.6 (2)
Rh–Fe–C27	166.1 (2)	C13–P2–C20	100.9 (2)
Rh–Fe–C28	66.6 (1)	C14–P2–C20	102.4 (2)
Rh–Fe–Si	76.41 (4)	O5–Si–O6	106.7 (2)
P2–Fe–C26	94.6 (1)	O5–Si–O7	108.4 (2)
P2–Fe–C27	95.2 (2)	O6–Si–O7	101.5 (2)
P2–Fe–C28	93.9 (1)	Si–O5–C30	126.6 (4)
P2–Fe–Si	174.65 (5)	Si–O6–C31	124.9 (3)
C26–Fe–C27	110.1 (2)	Si–O7–C32	126.8 (3)
C26–Fe–C28	138.8 (2)		

[a] Numbers in parentheses are estimated standard deviations in the least significant digits.

(13) (a) Antonelli, D. M.; Cowie, M. *Inorg. Chem.* **1990**, *29*, 4039. (b) Antonelli, D. M.; Cowie, M. *Organometallics* **1990**, *9*, 1818. (c) Hilts, R. W.; Franchuk, R. A.; Cowie, M. *Ibid.* **1991**, *10*, 304.

(14) (a) Dunbar, K. R.; Haefner, S. C.; Pence, L. E. *J. Am. Chem. Soc.* **1989**, *111*, 5504. (b) Cotton, F. A; Eagle, C. T.; Price, A. C. *Inorg. Chem.* **1988**, *27*, 4362. (c) Branan, D. M.; Hoffman, N. W.; McElroy, E. A.; Prokopuk, N.; Salazar, A. B.; Robbins, M. J.; Hill, W. E.; Webb, T. R. *Ibid.* **1991**, *30*, 1200.

(15) Caddy, P.; Green, M.; Howard, J. A. K.; Squire, J. M.; White, N. J. *J. Chem. Soc., Dalton Trans.* **1981**, 400.

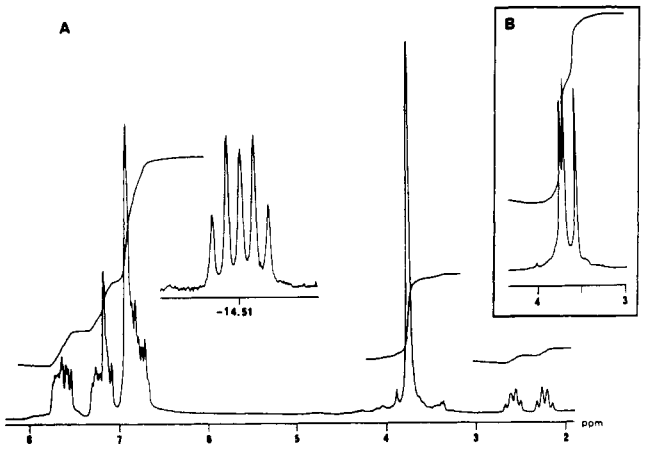

Figure 3. ^1H NMR spectrum of $[Fe(CO)_2\{\mu\text{-}Si(OMe)_2(OMe)\}(\mu\text{-dppm})(\mu\text{-}H)(\mu\text{-}CO)RhI]$ (**6c**): (A) at 298 K in benzene-d_6; (B) at 253 K in toluene-d_8 for the methoxy protons.

oxidation states (+I) and (0), respectively, in agreement with their coordination geometry. A number of mixed-metal complexes of the type $Rh(\mu\text{-dppm})_2M$ have been reported recently.[13]

Dynamic Behavior of the Fe–Rh Complexes. ^1H NMR studies of **1a** showed that the complex is rigid at room temperature as two methoxy resonances are observed in a 1:2 ratio at δ 3.74 and 3.89 in benzene-d_6 or at δ 3.90 and 3.70 in acetone-d_6, respectively. Similarly for **1b**, two types of OCH_2 groups are observed, giving rise to a broad quartet at δ 4.15 and a multiplet centered at δ 4.30 (AB part of an ABX_3 spin system) in a 1:2 ratio. The CH_3 protons all resonate at δ 1.40 (t, J(HH) = 7.1 Hz). In complex **3**, there are still two sets of resonances in a 1:2 ratio at δ 3.62 and 3.95 in benzene-d_6. Broadening of these signals is observed with increasing the temperature, until coalescence is reached at 343 K (δ 3.89, close to the weighted average between these chemical shifts of δ 3.84), what corresponds to an activation energy of ΔG^* = 70.1 kJ·mol^{-1}.[16] In complex **2**, the resonances at δ 4.09 and 2.77 (2:1 ratio) are sharp at 288 K and broaden at room temperature whereas the signals for the PCH_2P and aromatic protons remain sharp. Coalescence of the methoxy signals is observed around 328 K, corresponding to ΔG^* = 63.1 kJ·mol^{-1}. Sample decomposition occurred above this temperature. These trends are consistent with an increasing lability of the O→Rh dative interaction with the donor capacity of the ligand L attached to Rh in the sequence CO < $P(OPh)_3$ < PPh_3.

In the series of hydrido-bridged neutral complexes $Fe(CO)_2\{\mu\text{-}Si(OMe)_2(OMe)\}(\mu\text{-dppm})(\mu\text{-}H)(\mu\text{-}CO)RhX$ (**6a**, X = Cl; **6b**, X = Br; **6c**, X = I), a similar trend is observed. Thus, at room temperature in benzene-d_6, the methoxy resonance in **6a** is a broad singlet at δ 3.92 ($\Delta\nu_{1/2} \approx 20$ Hz), which appears at δ 3.70 ($\Delta\nu_{1/2} \approx 10$ Hz) in **6b** and at δ 3.76 ($\Delta\nu_{1/2} \approx 7$ Hz) in **6c**. The exchange rate thus increases along the series Cl < Br < I and parallels the increase in electron density at rhodium. At 253 K, the resonances for the methoxy protons in **6c** appear as three singlets of relative intensities 1:1:1 (see Figure 3) owing to chemical and magnetic inequivalence resulting from the presence of bridging H and CO ligands. The resonance of the μ-H ligand remains a doublet of triplets in the temperature range 253–300 K, indicating that this ligand retains its bridging nature throughout. The resonances at δ 3.72 and 3.68 coalesce around 273 K whereas further coalescence with the resonance at δ 3.55 occurs at 288 K, all methoxy protons becoming then equivalent and giving rise to a singlet at δ 3.68, corresponding to a ΔG^* value of ca. 60 kJ·mol^{-1} (Figure 3).

A similar situation is found for **5** in CD_2Cl_2 at 243 K where three singlets are observed for the methoxy protons at 3.68, 3.62 and 2.35 ppm. The first two resonances correspond to the uncoordinated methoxy groups and coalesce around 273 K (δ 3.67) whereas coalescence of all methoxy resonances then occurs at 298 K. These data are consistent with a strengthening of the Rh–oxygen interaction in the positively charged complexes.

Experimental Section

All reactions were performed in Schlenk-type flasks under purified nitrogen. Solvents were dried and distilled under nitrogen before use: tetrahydrofuran over sodium benzophenone–ketyl; toluene, benzene, and hexane over sodium; dichloromethane from P_2O_5. Nitrogen (Air Liquide R grade) was passed through BASF R3-11 catalyst and molecular sieve columns to remove residual oxygen and water. Column chromatography was performed under nitrogen with degassed silica gel. Elemental C and H analyses were performed by the Service Central de Microanalyses du CNRS. Infrared spectra were recorded in the region 4000–400 cm^{-1} on a Perkin-Elmer 398 spectrophotometer. The ^1H and $^{31}P\{^1H\}$ NMR spectra were recorded at 200.13 and 81.02 MHz, respectively, on a FT Brucker WP 200 SY instrument. Proton chemical shifts are positive downfield relative to external Me_4Si; $^{31}P\{^1H\}$ NMR spectra were externally referenced to 85% H_3PO_4 in H_2O with downfield chemical shift reported as positive. Mass spectra were measured on a Thompson THN 208 spectrometer (Université Louis Pasteur). The reactions were generally monitored by IR in the ν(CO) region. $[Fe(CO)_3\{Si(OMe)_2(OMe)\}(\mu\text{-dppm})Rh(CO)]$ (**1a**) was prepared as described previously[2] or by following the procedure detailed below for **1b**.

Synthesis of $[Fe(CO)_3\{Si(OEt)_2(OEt)\}(\mu\text{-dppm})Rh(CO)]$ (1b). A solution of $K[Fe(CO)_3\{Si)OEt)_3\}(dppm\text{-}P)]$[1] (0.727 g, 1.0 mmol) in THF (25 mL) was added to a solution of $[Rh(\mu\text{-Cl})(CO)_2]_2$ (0.194 g, 0.5 mmol) in THF (5 mL) at 0 °C. The reaction reaction mixture was stirred for 1 h at room temperature, and the solvent was removed under vacuum. The residue was extracted with Et_2O, and the orange solution was filtered and concentrated to ca. 5 mL. Addition of hexane (15 mL) induced precipitation of the product. After being stored overnight at −20 °C, the bright yellow, air-stable solid was filtered off and dried under vacuum (0.588 g, 72% yield). Anal. Calcd for $C_{35}H_{37}FeO_7P_2RhSi$ (M = 817.01): C, 51.43; H, 4.44. Found: C, 51.29; H, 4.50. IR (cyclohexane): ν(CO) 1982 s, 1959 vs, 1907 s, 1876 s cm^{-1}. ^1H NMR (200 MHz, benzene-d_6): δ 1.40 (t, 9 H, CH_3, ^3J(HH) = 7.1 Hz), 3.58 (dt, 2 H, PCH_2, ^2J(PH) = 10.2 Hz, ^3J(RhH) = 1 Hz), 4.15 (br q, 2 H, $RhOCH_2$, ^3J(HH) = 7.1 Hz), 4.30 (m, AB part of an ABX_3 spin system, 4 H, OCH_2, J(AB) ≈ 13 Hz), 6.87–7.76 (m, 20 H, C_6H_5). $^{31}P\{^1H\}$ NMR (81.02 MHz, acetone-d_6/CH_2Cl_2): δ 58.4 (d, P(Fe), ^{2+3}J(PP) = 66 Hz), 50.8 (dd, P(Rh), ^1J(RhP) = 177 Hz, ^{2+3}J(PP) = 66 Hz).

Synthesis of $[Fe(CO)_3\{Si(OMe)_2(OMe)\}(\mu\text{-dppm})Rh(PPh_3)]$ (2). Method A. A solution of $K[Fe(CO)_3\{Si(OMe)_3\}(dppm\text{-}P)]$ (0.343 g, 0.5 mmol) in THF (20 mL) was added to a solution of $[RhCl(PPh_3)_3]$ (0.463 g, 0.5 mmol) in THF (5 mL) at 0 °C. The reaction mixture was stirred for 1 h at room temperature, and then the solvent was removed under vacuum. The residue was extracted with toluene, and the orange solution was filtered and concentrated to ca. 5 mL. Addition of hexane (10 mL) induced precipitation of the product. The orange, air-stable solid was filtered off and dried under vacuum (0.505 g, 80% yield). Anal. Calcd for $C_{49}H_{46}FeO_6P_3RhSi$ (M = 1010.70): C, 58.23; H, 4.59. Found: C, 58.07; H, 4.51. IR (toluene): ν(CO) 1935 s, 1879

(16) ΔG^* values for exchange processes observed via NMR spectroscopy were calculated by using the Eyring equation; see: Günther, H. *NMR-Spektroskopie*; Georg Thieme Verlag: Stuttgart, 1983; Chapter 8.

m, 1830 m cm^{-1}. ^1H NMR (200 MHz, $CDCl_3$, 218 K): δ 2.36 (s, 3 H, $RhOCH_3$), 3.22 (t, 2 H, CH_2, $^2J(PH)$ = 10 Hz), 3.78 (s, 6 H, OCH_3), 7.03–7.66 (m, 35 H, C_6H_5), $^{31}P\{^1H\}$ NMR (81.02 MHz, acetone-d_6/CH_2Cl_2): δ 58.3 (dd, P1(Fe), ^{2+3}J(P1P2) = 61 Hz, ^3J(P1P3) = 6 Hz), 54.4 (ddd, P2(Rh), ^1J(RhP2) = 208 Hz, ^{2+3}J(P2P1) = 61 Hz, ^2J(P2P3) = 35 Hz), 29.8 (ddd, P3(Rh), ^1J(RhP3) = 175 Hz, ^2J(P3P2) = 35 Hz, ^3J(P3P1) = 6 Hz) (the ABMX pattern was analyzed in the first-order approximation).

Method B. To a solution of [HFe(CO)$_3${Si(OMe)$_3$}(dppm-*P*)] (0.129 g, 0.2 mmol) in toluene (6 mL) was added [HRh(CO)(PPh$_3$)$_3$] (0.184 g, 0.2 mmol). IR monitoring of the clear solution indicated quantitative formation of **1a** after 0.5 h. After 3 h, IR and $^{31}P\{^1H\}$ NMR spectroscopy showed complete conversion to complex **2**.

Method C. To a solution of [HFe(CO)$_3${Si(OMe)$_3$}(dppm-*P*)] (0.064 g, 0.1 mmol) in toluene (5 mL) was added [HRhCl{Si(OMe)$_3$}(PPh$_3$)$_2$] (0.078 g, 0.1 mmol). ($^{31}P\{^1H\}$ NMR (81.02 MHz, benzene-d_6/CH_2Cl_2): δ 40.5 (d, ^1J(RhP) = 120 Hz). After the reaction mixture was stirred for 3 h, $^{31}P\{^1H\}$ NMR spectroscopy showed nearly complete conversion to complex **2**.

Synthesis of [Fe(CO)$_3${Si(OMe)$_2$(OMe)}(μ-dppm)Rh{P(OPh)$_3$}] (3). To a stirred solution of **2** (0.253 g, 0.25 mmol) in toluene (10 mL) was added P(OPh)$_3$ (0.093 g, 0.3 mmol). After the clear orange solution was stirred for 0.5 h, the solvent was removed under vacuum. Addition of hexane (10 mL) to the oily residue caused solidification of **3** after vigorous stirring. The orange-yellow solid was filtered off and dried in vacuo (0.240 g, 91% yield). Anal. Calcd for $C_{49}H_{46}FeO_9P_3RhSi$ (M = 1058.66): C, 55.60; H, 4.38. Found: C, 57.00; H, 4.41. IR (toluene) ν(CO): 1952 s, 1884 m, 1857 m cm^{-1}. ^1H NMR (200 MHz, benzene-d_6): δ 3.47 (t, 2 H, CH_2, $^2J(PH)$ = 9.7 Hz), 3.62 (s, 3 H, $RhOCH_3$), 3.96 (s, 6 H, OCH_3), 6.63–7.39 (m, 35 H, C_6H_5). $^{31}P\{^1H\}$ NMR (81.02 MHz, benzene-d_6/CH_2Cl_2): δ 102.5 (ddd, P3(OPh)$_3$, ^1J(RhP3) = 307 Hz, ^2J(P2P3) = 44 Hz, ^3J(P1P3) = 11 Hz), 59.0 (dd, P1(Fe), ^{2+3}J(P1P2) = 61 Hz, ^3J(P1P3) = 11 Hz), 52.55 (ddd, P2(Rh), ^1J(RhP2) = 196 Hz, ^{2+3}J(P1P2) = 61 Hz, ^2J(P2P3) = 44 Hz).

Synthesis of [Fe(CO)$_3${Si(OMe)$_3$}(μ-dppm)Rh(CO)$_2$] (4). Carbon monoxide was bubbled through a solution of [Fe(CO)$_3${μ-Si(OMe)$_2$(OMe)}(μ-dppm)Rh(CO)] (**1**) (0.194 g, 0.25 mmol) in dichloromethane (5 mL). Hexane (2 mL) was added when the volume of the solution was reduced to ca. 1 mL, and bubbling was continued for 10 min. Cooling to −30 °C afforded a white solid. The solvent was syringed off, and the solid was dried under carbon monoxide (0.151 g, 75% yield). Anal. Calcd for $C_{33}H_{31}FeO_8P_2RhSi$ (M = 804.39): C, 49.27; H, 3.88. Found: C, 49.35; H, 3.77. IR (cyclohexane): ν(CO) 2051 m, 1995 m, 1980 s, 1947 s, 1931 s cm^{-1}. ^1H NMR (200 MHz, toluene-d_8, 298 K): δ 3.55 (s, 9 H, OCH_3), 3.94 (t, 2 H, CH_2, $^2J(PH)$ = 8.8 Hz), 6.90–7.64 (m, 20 H, C_6H_5). ^1H NMR (200 MHz, toluene-d_8, 253 K): δ 3.55 (s, 9 H, OCH_3). $^{31}P\{^1H\}$ NMR (81.02 MHz, acetone-d_6/CH_2Cl_2, 253 K): δ 65.3 (s, P(Fe)), 15.5 (d, P(Rh), ^1J(RhP) = 81 Hz).

Synthesis of [Fe(CO)$_2${Si(OMe)$_2$(OMe)}(μ-dppm)(μ-H)(μ-CO)Rh(PPh$_3$)][BF$_4$] (5). To a stirred solution of **2** (0.253 g, 0.25 mmol) in dichloromethane (10 mL) at −40 °C was added a diethyl ether solution of HBF_4 in excess. After the clear orange solution was stirred for 0.3 h, the solvent was removed under vacuum. The yellow solid was washed with hexane and dried in vacuo (0.247, 90% yield). Anal. Calcd for $C_{49}H_{47}FeO_6P_2RhSiBF_4$ (M = 1098.5): C, 53.58; H, 4.31. Found: C, 52.40; H, 4.32. Mass spectrum (FAB$^+$): 1011 (M^+ − BF_4, 85%). IR (CH_2Cl_2): ν(CO) 2034 s, 1986 s, 1827 m cm^{-1}. ^1H NMR (200 MHz, $CDCl_3$, 243 K): δ −14.20 (m, 1 H, FeHRh), 2.35 (s, 3 H, $RhOCH_3$), 3.2 (br, 2 H, PCH_2), 3.62 (s, 3 H, OCH_3), 3.68 (s, 3 H, OCH_3), 6.80–7.60 (m, 35 H, C_6H_5). $^{31}P\{^1H\}$ NMR (81.02 MHz, acetone-d_6/CH_2Cl_2): δ 49.7 (br dm, P2(Rh), ^1J(RhP2) = 161 Hz, ^{2+3}J(P1P2) = 51 Hz, ^2J(P2P3) = 35 Hz), 38.4 (d, P1(Fe), ^{2+3}J(P1P2) = 51 Hz), 20.6 (br dm, P3(Rh), ^1J(RhP3) = 132 Hz, ^2J(P2P3) = 35 Hz, ^3J(P1P3) not determined).

Synthesis of [Fe(CO)$_2${Si(OMe)$_2$(OMe)}(μ-dppm)(μ-H)(μ-CO)RhCl] (6a). Solid [HFe(CO)$_3${Si(OMe)$_3$}(dppm-*P*)] was added to a suspension of [Rh$_2$(μ-Cl)$_2$(COD)$_2$] (0.123 g, 0.25 mmol) in diethyl ether (10 mL). The reaction mixture was stirred for 0.5 h. Addition of hexane induced precipitation of an orange solid that was collected by filtration and dried in vacuo (0.353 g, 95%). Anal. Calcd for $C_{31}H_{32}ClFeO_6P_2RhSi$ (M = 784.83): C, 47.44; H, 4.11. Found: C, 47.20; H, 4.25. IR (CH_2Cl_2): ν(CO) 2014 s, 1965 s, 1793 m cm^{-1}. ^1H NMR (200 MHz, CD_2Cl_2, 233 K): δ −16.28 (m, 1 H, FeHRh), 2.61 (m, 2 H, CH_2), 3.41 (s, 3 H, $RhOCH_3$), 3.62 (s, 3 H, OCH_3), 3.65 (s, 3 H, OCH_3), 7.15–7.60 (m, 20 H, C_6H_5). ^1H NMR (200 Hz, benzene-d_6, 298 K): δ −15.86 (dt, 1 H, FeHRh, ^1J(RhH) = 26.2 Hz, $^2J(PH)$ = 15.1 Hz), 2.08 and 2.39 (aspect of two broadened quartets with line separations of ca. 12 Hz, 2 H, CH_2), 3.67 (s br, 9 H, OCH_3), 6.68–7.82 (m, 20 H, C_6H_5), $^{31}P\{^1H\}$ NMR (81.02 MHz, benzene-d_6/CH_2Cl_2): δ 52.5 (dd, P(Rh), ^1J(RhP) = 156 Hz, ^{2+3}J(PP) = 56 Hz), 49.7 (d, P(Fe), ^{2+3}J(PP) = 56 Hz).

Synthesis of [Fe(CO)$_2${Si(OMe)$_2$(OMe)}(μ-dppm)(μ-H)(μ-CO)RhI] (6c). Solid **6a** (0.196 g, 0.25 mmol) was added to a suspension of NaI (0.6 g, 4 mmol) in THF (10 mL), and the mixture was stirred for 0.5 h. The suspension was filtered, and the resulting red solution was concentrated to ca. 5 mL and layered with hexane. After a few days at −15 °C, red microcrystals of the product were formed and collected (0.175 g, 80% yield). Anal. Calcd for $C_{31}H_{32}FeIO_6P_2RhSi$ (M = 876.28): C, 42.45; H, 3.68. Found: C, 44.65; H, 3.89. IR (toluene): ν(CO) 2011 s, 1963 s, 1788 m cm^{-1}. ^1H NMR (200 MHz, toluene-d_8, 253 K): δ −14.67 (dt, 1 H, FeHRh, ^1J(RhH) = 27.8 Hz, $^2J(PH)$ = 15.0 Hz), 1.90 and 2.33 (aspect of two broadened quartets with line separations of ca. 12 Hz, 2 H, CH_2), 3.55 (s, 3 H, $RhOCH_3$), 3.68 (s, 3 H, OCH_3), 3.72 (s, 3 H, OCH_3), 6.53–7.49 (m, 20 H, C_6H_5). ^1H NMR (200 Hz, benzene-d_6, 298 K): δ −14.51 (dt, 1 H, FeHRh, ^1J(RhH) = 27.7 Hz, $^2J(PH)$ = 15.0 Hz), 2.24 (m, 1 H, CH_2), 2.59 (m, 1 H, CH_2), 3.76 (s, 9 H, OCH_3), 6.71–7.74 (m, 20 H, C_6H_5). $^{31}P\{^1H\}$ NMR (81.02 MHz, benzene-d_6/CH_2Cl_2): δ 50.85 (dd, P(Rh), ^1J(RhP) = 155 Hz, ^{2+3}J(PP) = 55 Hz), 44.15 (d, P(Fe), ^{2+3}J(PP) = 55 Hz).

Reaction of [Fe(CO)$_2${Si(OMe)$_2$(OMe)}(μ-dppm)(μ-H)(μ-CO)RhCl] with CO. A solution of **6a** (0.101 g, 0.1 mmol) in benzene-d_6 was purged with CO for 6 min. ^1H and $^{31}P\{^1H\}$ NMR monitoring showed complete conversion to the hydrido complex **7**. ^1H NMR (200 MHz, benzene-d_6, 298 K): δ −6.41 (ddd, 1H, RhH, ^1J(RhH) = 21.9 Hz, $^2J(PH)$ = 10 and 5.9 Hz), 3.78 (s, 9 H, OCH_3), 4.34 (t, 2 H, CH_2, $^2J(PH)$ = 12 Hz), 6.81–7.64 (m, 20 H, C_6H_5). $^{31}P\{^1H\}$ NMR (81.02 MHz, benzene-d_6/CH_2Cl_2): δ 63.1 (d, P(Fe), ^{2+3}J(PP) = 73 Hz), 44.8 (dd, P(Rh), ^1J(RhP) = 148 Hz, ^{2+3}J(PP) = 73 Hz).

Synthesis of [Fe(CO)$_3${Si(OMe)$_3$}(μ-dppm)Rh(CS)(PPh$_3$)] (8). A solution of K[Fe(CO)$_3${Si(OMe)$_3$}(dppm-*P*)] (0.343 g, 0.5 mmol) in THF (20 mL) was added to a suspension of [RhCl(CS)(PPh$_3$)$_2$][11] (0.353 g, 0.5 mmol) in THF (5 mL) at 0 °C. The clear orange-red reaction mixture was stirred for 1 h at room temperature and filtered, and then the solvent was removed under vacuum. The residue was extracted with CH_2Cl_2, and the orange solution was filtered and concentrated to ca. 5 mL. Addition of hexane (10 mL) induced precipitation of the product. The orange, air-stable solid was filtered off and dried in vacuum (0.445 g, 78% yield). Anal. Calcd for $C_{50}H_{46}FeO_6P_3RhSSi{\cdot}CH_2Cl_2$ (M = 1139.67): C, 53.75; H, 4.25; P, 8.15; S, 2.81. Found: C, 54.53; H, 4.28; P, 8.15; S, 3.04. Mass spectrum (FAB$^+$): 1054 (M^+, 1%), 1026 (M^+ − CO, 2%), 998 (M^+ − 2CO, 8%), 970 (M^+ − 3CO, 67%). IR (CH_2Cl_2): ν(CO) 1979 s, 1946 s, 1892 m, ν(CS) 1190 w cm^{-1}. ^1H NMR (200 MHz, benzene-d_6): δ 3.22 (t, 2 H, CH_2, $^2J(PH)$ = 10 Hz), 3.62 (s, 9 H, OCH_3), 6.60–7.79 (m, 35 H, C_6H_5). $^{31}P\{^1H\}$ NMR (161.99 MHz, benzene-d_6/CH_2Cl_2): δ 52.5 (ddd, P1(Fe), ^{2+3}J(P1P2) = 82 Hz, ^3J(P1P3) = 18 Hz, ^2J(P1Rh) = 1 Hz), 21.2 (ddd, P3(Rh), ^1J(RhP3) = 134 Hz, ^2J(P2P3) = 12 Hz), ^3J(P3P1) = 18 Hz), 20.3 (ddd, P2(Rh), ^1J(RhP2) = 129 Hz, ^2J(P3P2) = 12 Hz, ^{2+3}J(P2P1) = 82 Hz).

Reaction of K[Fe(CO)$_3${Si(OMe)$_3$}(dppm-*P*)] with [IrCl(CO)(PPh$_3$)$_2$]. A solution of K[Fe(CO)$_3${Si(OMe)$_3$}(dppm-*P*)] (0.343 g, 0.5 mmol) in THF (20 mL) was added to a suspension of [IrCl(CO)(PPh$_3$)$_2$] (0.353 g, 0.5 mmol) in THF (5 mL) at 20 °C. The reaction mixture was stirred for 3 h at room termperature

Table III. X-ray Data Collection Parameters for [Fe(CO)$_3${μ-Si(OMe)$_2$(OMe)}(μ-dppm)Rh(CO)] (1a)

formula	$C_{33}H_{33}O_7SiP_2Cl_2FeRh$
molecular weight	861.32
color	yellow-orange
crystal system	monoclinic
a (Å)	22.717 (5)
b (Å)	11.348 (2)
c (Å)	14.202 (2)
β (deg)	94.47
V (Å^3)	3650.2
Z	4
D_{calc} (g cm^{-3})	1.567
space group	$P2_1/n$
radiation	Mo Kα (graphite monochromated)
wavelength (Å)	0.709 30
μ (cm^{-1})	11.516
crystal size (mm)	0.22 × 0.29 × 0.33
temperature (°C)	22
diffractometer	Enraf-Nonius CAD4-F
mode	$\theta/2\theta$
scan speed (deg s^{-1})	variable
scan width (deg)	1.00 + 0.343 tan θ
θ limits (deg)	2/25
octants	$\pm h,+k,+l$
no. of data collected	7040
no. of data with $I > 3\sigma(I)$	4531
abs min/max	0.85/1.12
no. of parameters refined by LS	424
$R(F)$	0.033
$R_w(F)$	0.052
p	0.08
GOF	1.095

until the IR absorptions due to K[Fe(CO)$_3${Si(OMe)$_3$}(dppm-P)] had disappeared. During this time, the color of the solution changed from yellow to orange-brown. After filtration of the reaction mixture, the solvent was removed under vacuum and the residue was examined by $^{31}P\{^1H\}$ NMR and IR spectroscopies, which revealed the presence of [Fe(CO)$_3$(PPh$_3$)(dppm-P)] as the main product in the reaction mixture (ca. 65% from integration of the ^{31}P NMR resonances). This bright yellow, air-stable compound was crystallized by layering a concentrated THF solution of the reaction mixture with hexane (0.330 g, 42% yield). Anal. Calcd for $C_{46}H_{37}FeO_3P_3$ (M = 786.57): C, 70.24; H, 4.74; Fe, 7.10; P, 11.81. Found: C, 68.96; H, 4.67; Fe, 6.86; P, 11.41. IR (CH_2Cl_2): ν(CO) 1884 s, 1880 s, sh cm^{-1}. IR (KBr): ν(CO) 1875 vs, cm^{-1}. ^1H NMR (200 MHz, benzene-d_6): δ 3.69 (d, 2 H, CH_2, ^2J(PH) = 8.3 Hz), 3.62 (s, 9 H, OCH_3), 7.16–7.96 (m, 35 H, C_6H_5). $^{31}P\{^1H\}$ NMR (81.02 MHz, acetone-d_6/CH_2Cl_2): δ 82.3 (d, PPh_3(Fe), ^2J(P1P2) = 32 Hz), 75.9 (dd, dppm-P2(Fe), ^2J(P2P3) = 75 Hz, ^2J(P2P1) = 32 Hz), -24.8 (d, P3(uncoord), ^2J(P3P2) = 75 Hz).

Crystal Structure Determination of 1a·CH_2Cl_2. Suitable crystals were obtained from CH_2Cl_2/hexane solutions at 0 °C. A single crystal was cut out from a cluster of crystals and mounted on a rotation-free goniometer head. A systematic search in reciprocal space using a Enraf-Nonius CAD4-F automatic diffractometer showed that crystals of 1a·CH_2Cl_2 belong to the monoclinic system. Quantitative data were obtained at room temperature. All experimental parameters used are given in Table III. The resulting data set was transfered to a VAX computer, and for all subsequent calculations the Enraf-Nonius SDP/VAX package[17] was used. Three standard reflections measured every hour during the entire data collection period showed no significant trend. The raw data were converted to intensities and corrected for Lorentz, polarization, and absorption factors, the latter derived from ψ scans. The structure was solved by the heavy-atom method. After refinement of the heavy atoms, a difference Fourier map revealed maxima of residual electronic density close to the positions expected for hydrogen atoms; they were introduced in structure factor calculations by their computed coordinates (C–H = 0.95 Å) and isotropic temperature factors such as B(H) = 1.3 B_{eq}(C) Å^2 but not refined. Full least-squares refinements: $\sigma^2(F^2)$ = σ^2(counts) + $(pI)^2$. A final difference map revealed no significant maxima. Atomic coordinates are given in Table IV. The scattering factor coefficients and anomalous dispersion coefficients come from ref 18, parts a and b, respectively.

Table IV. Positional Parameters (Esd's in Parentheses) for [Fe(CO)$_3${μ-Si(OMe)$_2$(OMe)}(μ-dppm)Rh(CO)] (1a)

atom	x	y	z	B^a (Å^2)
Rh	0.43330 (1)	0.05059 (3)	0.17242 (2)	2.766 (6)
Fe	0.49186 (2)	0.20557 (5)	0.28068 (4)	2.54 (1)
P1	0.34861 (5)	0.1404 (1)	0.18382 (8)	2.74 (2)
C1	0.3040 (2)	0.1546 (4)	0.0717 (3)	3.04 (9)
C2	0.3258 (2)	0.2229 (4)	0.0018 (3)	3.8 (1)
C3	0.2943 (3)	0.2373 (5)	−0.0846 (4)	4.7 (1)
C4	0.2402 (2)	0.1819 (5)	−0.1019 (4)	4.9 (1)
C5	0.2191 (2)	0.1119 (5)	−0.0342 (4)	5.2 (1)
C6	0.2513 (2)	0.0976 (5)	0.0532 (4)	4.3 (1)
C7	0.2993 (2)	0.0797 (4)	0.2656 (3)	3.37 (9)
C8	0.2459 (2)	0.1317 (4)	0.2796 (4)	4.3 (1)
C9	0.2105 (2)	0.0929 (5)	0.3495 (5)	5.3 (1)
C10	0.2304 (3)	−0.0022 (5)	0.4046 (4)	5.3 (1)
C11	0.2826 (3)	−0.0588 (5)	0.3898 (4)	4.9 (1)
C12	0.3168 (2)	−0.0178 (4)	0.3199 (4)	3.7 (1)
C13	0.3562 (2)	0.2957 (4)	0.2210 (3)	2.82 (8)
P2	0.41660 (5)	0.31890 (9)	0.31217 (8)	2.48 (2)
C14	0.3852 (2)	0.3022 (4)	0.4253 (3)	3.08 (9)
C15	0.3262 (2)	0.3068 (5)	0.4362 (4)	4.2 (1)
C16	0.3049 (3)	0.2984 (6)	0.5254 (4)	5.7 (1)
C17	0.3426 (3)	0.2874 (6)	0.6021 (4)	6.5 (2)
C18	0.4024 (3)	0.2847 (6)	0.5939 (4)	6.1 (2)
C19	0.4227 (2)	0.2880 (6)	0.5056 (4)	5.0 (1)
C20	0.4266 (2)	0.4796 (4)	0.3043 (3)	2.83 (9)
C21	0.4136 (2)	0.5564 (4)	0.3741 (4)	4.2 (1)
C22	0.4420 (3)	0.6761 (5)	0.3655 (4)	5.4 (1)
C23	0.4433 (3)	0.7209 (4)	0.2851 (5)	5.2 (1)
C24	0.4562 (3)	0.6459 (5)	0.2136 (4)	5.5 (1)
C25	0.4485 (2)	0.5240 (4)	0.2238 (4)	4.4 (1)
C26	0.4715 (2)	0.0871 (4)	0.3543 (3)	3.39 (9)
O1	0.4605 (2)	0.0110 (3)	0.4035 (3)	4.52 (8)
C27	0.5459 (2)	0.2938 (5)	0.3416 (4)	3.9 (1)
O2	0.5821 (2)	0.3512 (4)	0.3803 (3)	6.4 (1)
C28	0.4872 (2)	0.2430 (4)	0.1602 (3)	3.06 (9)
O3	0.4875 (2)	0.2757 (3)	0.0822 (2)	4.40 (8)
C29	0.3933 (2)	−0.0677 (4)	0.1061 (4)	4.2 (1)
O4	0.3670 (2)	−0.1425 (4)	0.0688 (3)	7.3 (1)
Si	0.56231 (5)	0.0802 (1)	0.24022 (9)	3.01 (2)
O5	0.6140 (1)	0.1377 (3)	0.1813 (3)	5.00 (8)
C30	0.6709 (2)	0.0908 (6)	0.1722 (5)	6.5 (2)
O6	0.5948 (2)	−0.0095 (3)	0.3171 (3)	4.29 (7)
C31	0.6260 (3)	0.0255 (6)	0.4035 (4)	5.9 (1)
O7	0.5229 (1)	−0.0139 (3)	0.1687 (2)	3.96 (7)
C32	0.5454 (3)	−0.1042 (5)	0.1126 (4)	5.5 (1)
C33	0.6164 (4)	0.4231 (8)	0.1359 (8)	16.0 (3)
CL1	0.5831 (1)	0.5134 (2)	0.0542 (2)	11.28 (7)
CL2	0.6908 (1)	0.4349 (2)	0.1560 (2)	13.34 (7)

[a] Anisotropically refined atoms are given in the form of the isotropic equivalent displacement parameter defined as: $^4/_3[a^2\beta(1,1) + b^2\beta(2,2) + c^2\beta(3,3) + ab(\cos\gamma)\beta(1,2) + ac(\cos\beta)\beta(1,3) + bc(\cos\alpha)\beta(2,3)]$.

Acknowledgment. Financial support from the CNRS (Paris), Deutsche Forschungsgemeinschaft (Bonn) (to M.K.), Ministerio de Educacion y Ciencia (Madrid) (to E.V.), and Commission of the European Communities (Contract No. ST2J-0347-C) is gratefully acknowledged.

Registry No. 1a, 133336-76-2; 1a·CH_2Cl_2, 136085-20-6; 1b, 135929-07-6; 2, 135952-61-3; 3, 135929-04-3; 4, 135929-05-4; 5, 135952-63-5; 6a, 135952-64-6; 6c, 135929-08-7; 7, 135952-65-7; 8, 135929-06-5; [Fe(CO)$_3$(PPh$_3$)(dppm-P)], 135929-09-8; K[Fe(CO)$_3${Si(OEt)$_3$}(dppm-P)], 135745-70-9; K[Fe(CO)$_3${Si(OMe)$_3$}(dppm-P)], 123674-03-3; [Rh(μ-Cl)(CO)$_2$]$_2$, 14523-22-9; [RhCl(PPh$_3$)$_3$], 14694-95-2; [HRh(CO)(PPh$_3$)$_3$], 17185-29-4; [HRhCl{Si(OMe)$_3$}(PPh$_3$)$_2$], 135929-10-1; [Rh$_2$(μ-Cl)$_2$(COD)$_2$], 12092-47-6;

(17) Frenz, B. A. *The Enraf-Nonius CAD4-SDP.* In *Computing in Crystallography*; Schenk, H., Olthof-Hazekamp, R., Van Koningveld, H., Bassi, G. C., Eds.; Delft University Press: Delft, 1978; pp 64–71.

(18) Cromer, D. T.; Waber, J. T. *International Tables for X-ray Crystallography*; Kynoch Press: Birmingham, England, 1974; Vol. IV: (a) Table 2.2b; (b) Table 2.3.1.

[RhCl(CS)(PPh_3)$_2$], 26500-10-7; [IrCl(CO)(PPh_3)$_2$], 14871-41-1; Fe, 7439-89-6; Rh, 7440-16-6.

Supplementary Material Available: Tables of temperature factors for anisotropic atoms (S-I), hydrogen atom positional parameters (S-II), bond distances (S-III), and bond angles (S-IV) (8 pages); a listing of observed and calculated structure factor amplitudes (×10) for all observed reflections (S-V) (17 pages). Ordering information is given on any current masthead page.

Allene Adducts of Ditungsten Hexaalkoxides. Three Modes of Allene Coordination to Dinuclear Centers As Seen in the Structures of W_2(O-*t*-Bu)$_6$(C_3H_4), W_2(O-*t*-Bu)$_6$(C_3H_4)$_2$, and W_2(O-*t*-Bu)$_6$(C_3H_4)(CO)$_2$

Stephanie T. Chacon, Malcolm H. Chisholm,* Kirsten Folting, John C. Huffman, and Mark J. Hampden-Smith

Department of Chemistry and Molecular Structure Center, Indiana University, Bloomington, Indiana 47405

Received April 5, 1991

Hydrocarbon solutions of W_2(O-*t*-Bu)$_6$ and allene (1 equiv) react at 0 °C to give the monoallene adduct W_2(O-*t*-Bu)$_6$(C_3H_4) (1). Reactions involving W_2(O-*t*-Bu)$_6$ and an excess of allene (>10 equiv) yield the 2:1 adduct W_2(O-*t*-Bu)$_6$(C_3H_4)$_2$ (2). Compound 1 reacts with allene (>10 equiv) and CO (>2 equiv) to yield 2 and W_2(O-*t*-Bu)$_6$(C_3H_4)(CO)$_2$ (3), respectively. A monoallene adduct involving methylallene and W_2(O-*t*-Bu)$_6$ has also been prepared, but reactions involving other W_2(OR)$_6$ compounds where R = *i*-Pr, *c*-Hex, *c*-Pen, and CH_2-*t*-Bu all yield 2:1 adducts, W_2(OR)$_6$(C_3H_4)$_2$. The molecular structures of 1–3 have been determined by low-temperature single-crystal X-ray crystallography. Crystal data for 1: monoclinic, $P2_1/n$, a = 11.676 (1) Å, b = 16.771 (2) Å, c = 17.116 (2) Å, β = 90.39 (0)°, Z = 4. For 2: monoclinic, $P2_1/c$, a = 9.516 (3) Å, b = 19.114 (7) Å, c = 19.438 (6) Å, β = 103.32 (2)°, Z = 4. For 3: monoclinic, $P2_1/c$, a = 15.823 (4) Å, b = 18.807 (5) Å, c = 22.457 (6) Å, β = 90.93 (1)°, Z = 8. The monoallene adduct 1 has a μ-parallel-bridged allene with C–C–C = 141° and W–W = 2.583 (1) Å, W–CH_2 = 2.13 (1) Å, W–C = 2.09 (1) Å, and C–CH_2 = 1.47 (1) Å. This novel $W_2(\mu$-$C_3H_4)$ skeleton is supported by six terminal O-*t*-Bu ligands, three at each W center, W–O = 1.90 (2) Å (average). By contrast, the molecular structure of 2 shows a central $W_2(\mu$-η^1,η^3-$C_3H_4)$ group with an attendant η^2-allene ligand at one metal center. The W–W distance is 2.855 (1) Å and is supported by two bridging alkoxide ligands. The structure of 3 is related to that of 2 by the substitution of the terminal η^2-allene by two η^1-CO ligands. The W–W distance is 3.012 (4) Å, and the two O-*t*-Bu bridges are asymmetric with W–O = 1.99 (3) and 2.30 (4) Å (average), where the long W–O distances are trans to the CO ligands. The bonding in 3 may be viewed as W(6+)---W(2+) where the two CO ligands bond to a pseudooctahedral d^4 metal center. The present work complements earlier studies involving the reactions between W_2(OR)$_6$ compounds with ethylene and alkynes, and the bonding in these adducts has been investigated by qualitative and semiempirical MO approaches.

Introduction

Much of organometallic chemistry owes its existence to an inorganic template. One can think of the spectacular growth during the 1960s and '70s of the organometallic chemistry of the group 8–10 elements that exploited d^6, d^8, and d^{10} ML_n fragments for which tertiary phosphines and phosphites played a ubiquitous ancillary role. More recently, but equally spectacular, has been the organometallic chemistry supported by the d^0, d^2-bent Cp_2M and Cp^*_2M fragments. The work of Bercaw, Marks, and others with the early transition metals, the group 3 elements (Sc, Y), and the lanthanides and actinides has opened up an organometallic chemistry that had lain barren for decades and could not have been developed but for the use of Cp and Cp* ligands. Our efforts are aimed at developing organometallic chemistry of dinuclear systems containing M–M multiple bonds. A particularly attractive group of compounds has the formula M_2(OR)$_6$ where M = Mo and W and R = alkyl or aryl. These are coordinatively unsaturated, and the metal centers are Lewis acidic, yet the presence of the M≡M bond affords an electron reservoir for π-acid ligands and redox chemistry.[1] The selection of M, Mo vs W, and R influences both steric and electronic factors, and thus a M_2(OR)$_6$ compound can be made substrate selective. As part of our continuing investigations of the reactivity of W_2(OR)$_6$ compounds toward unsaturated organic molecules, we have examined reactions involving allene and methylallene. We describe herein our findings. Preliminary reports have appeared.[2,3]

Results and Discussion

Syntheses. W_2(O-*t*-Bu)$_6$ and allene (1 equiv) react in hexane at 0 °C to give W_2(O-*t*-Bu)$_6$(C_3H_4) (1), which crystallizes at −72 °C (dry ice/EtOH), as dark green blocks (cubes). Crystals suitable for an X-ray study were obtained from Et_2O at −72 °C. Compound 1 is thermally unstable in solution above 0 °C, and the decomposition products W_2(O-*t*-Bu)$_6$ and (*t*-BuO)$_3$W≡CMe[4] have been identified by NMR spectroscopy. Even in the crystalline state, compound 1 decomposes slowly (24 h) at room temperature, ca. 25 °C. However, when stored in the solid state at −20 °C it appears indefinitely stable, ca. 1 year. Com-

(1) Chisholm, M. H. *New. J. Chem.* **1987**, *6*, 459.

(2) Cayton, R. H.; Chisholm, M. H.; Hampden-Smith, M. J. *J. Am. Chem. Soc.* **1988**, *110*, 4438.

(3) Cayton, R. H.; Chacon, S. T.; Chisholm, M. H.; Hampden-Smith, M. J.; Huffman, J. C.; Folting, K.; Ellis, P. D.; Huggins, B. A. *Angew. Chem., Int. Ed. Engl.* **1989**, *28*, 11; *Angew. Chem.* **1989**, *101*, 1547.

(4) Listemann, M. L.; Schrock, R. R. *Organometallics* **1985**, *4*, 74.

0276-7333/91/2310-3722$02.50/0